Latin American Journal of Aquatic Research, 53(3): 473-487, 2025
DOI: 10.3856/vol53-issue3-fulltext-3368

Research Article

Climatology, trends, and atmospheric teleconnections of cold fronts in the Colombian Caribbean Sea from 1996 to 2021

Juan C. Ortiz[1], Humberto Llinás[2], Helber Gomes[3] & Matheus Lyra[3]
[1]Departamento de Física y Geociencias, Universidad del Norte, Barranquilla, Colombia
[2]Departamento de Matemáticas y Estadística, Universidad del Norte, Barranquilla, Colombia
[3]Instituto de Ciencias Atmosféricas, Universidad Federal de Alagoas, Maceió, Brasil
Corresponding author: Juan C. Ortiz (jortiz@uninorte.edu.co)

ABSTRACT. Cold fronts (Cfs) in the Caribbean Sea significantly impact the coastal regions of South America, generating extreme waves and causing severe damage, particularly during the winter season. This study aims to analyze the climatology, trends, and atmospheric teleconnections of Cfs in the Colombian Caribbean from 1996 to 2021, providing a comprehensive assessment of their frequency and variability. A total of 6 to 9 additional Cfs per year were identified compared to previous studies, indicating an increasing trend. The Dickey-Fuller test confirmed that the time series was non-stationary. In contrast, Kendall's test rejected the absence of a monotonic trend, supporting the existence of significant variations in Cfs occurrences. Regarding atmospheric teleconnections, the El Niño-Southern Oscillation (ENSO) and the Quasi-Biennial Oscillation (QBO) showed weak correlations with Cfs frequencies. However, a stronger correlation was found with the Pacific North American (PNA) pattern ($r = 0.42$, $P < 0.05$) and the North Atlantic Oscillation (NAO) ($r = 0.48$, $P < 0.05$), indicating a more pronounced influence of these large-scale circulation patterns. The frequency of Cfs activity was higher during El Niño events, the positive phase of the NAO and PNA, and the negative phase of the QBO, suggesting that these climate modes modulate the penetration of frontal systems into the region. Additionally, a detailed case study of a Cf event in January 2021 highlighted the development and progression of a baroclinic cyclone and its associated frontal system over the Colombian Caribbean. The system's core remained at low atmospheric levels, exhibiting intense westward flow and the presence of the Subtropical Jet Stream at upper levels, contributing to its intensification.

Keywords: cold fronts; climatology; atmospheric teleconnections; Caribbean Sea; Colombian coast

INTRODUCTION

Cold fronts (Cfs) in the northern hemisphere are normally accompanied by rainfall, causing floods and increasing winds and ocean waves (Locatelli et al. 1989, Beringer & Tepper 2000, Faustino-Eslava et al. 2011). The incursion of Cfs from mid-latitudes towards the Caribbean Sea is frequent during winter when the polar front is displaced towards the equator. In the case of the eastern tropical Pacific, Cfs first cross the Isthmus of Tehuantepec and continue to move southeastward, creating relatively high surface pressure a day or two later in the southwestern Caribbean Sea. The Earth's rotation contributes to the formation of depression-type storms that move along these fronts. These storms occur throughout the year at short time intervals, resulting in wave conditions that can vary on relatively short time scales with unpredictable patterns, as these fronts shift frequently in the north-south direction (Amador et al. 2006). Zárate (2013) analyzed 37 winter seasons in the Northern Hemisphere between 1975 and 2012, covering the period from November to

Associate Editor: Juan Placencia

February, including both cold air masses that entered with well-defined Cfs and those that only exhibited frontal shear lines. These incursions were referred to interchangeably as cold pushes, which is synonymous with cold air masses. In the span of 37 seasons, 600 cold air masses, which reached Central America and the Caribbean, were identified. When a winter cold air mass with deep latitudinal penetration passes through, the Caribbean Low-Level Jet (CLLJ) shows its maximum velocity in the Pacific branch when the meridional pressure gradient increases to a much greater degree in that area than in the Caribbean Sea. The increase in the intensity of the easterly wind over Central America during the first 2 or 3 days due to the passage of a cold air mass with deep latitudinal intrusion is preferably linked to the maximum wind that forms in the Pacific branch and not to the wind current coming from the Caribbean, which during that period tends to show lower speeds concerning the average monthly values.

The Mojave or Arizona Deserts are areas from where cold air masses begin their eastward motion, crossing warmer and more humid areas such as the Gulf of Mexico and occasionally the Caribbean Sea. Incursions of cold mid-latitude air that penetrate deep into the tropics are frequently observed to the east of major north-south oriented mountain ranges. The so-called cold surges are confined to the lower troposphere, exhibit horizontal scales ranging from 500 to 1,000 km, and can be traced over periods of 2 to 7 days. The passage of a cold surge is typically characterized by a rapid and marked decrease of air temperature and dew point at low levels, a sharp increase in surface pressure, and a day or so of moderate to strong equatorward low-level winds. The strong surface pressure gradient drives an equatorward geostrophic low-level wind that advects the cold air and dominates the local cooling. In turn, the cold air raises the surface pressure and strengthens the meridional pressure gradient (Garreaud 2001).

On the other hand, the intrusion of fronts in the Caribbean Sea can produce changes in the wind, pressure, and temperature fields, which are very well-defined initially in the Gulf of Mexico but weaken as the front advances towards the warm and humid waters of the Caribbean Sea (Narváez & León 2003). In the Colombian Caribbean basin, they usually arrive between November and April (Ortiz et al. 2013). Figure 1 shows the arrival of a Cf on February 20, 2024, displayed on a satellite image (GEOCOLOR Composite) and its corresponding surface map (this event was also reported in Instituto Meteorológico Nacional de Costa Rica-IMN 2024).

In the Colombian Caribbean Sea coast, the latitudinal migration of the Intertropical Convergence Zone (ITCZ) is the most important source of climate variability. There is a bimodal behavior in precipitation during which precipitation is scarce for one part of the year (December-March) and where precipitation increases for the other part of the year (April-November), with October being the wettest month of the year. Trade winds from the northeast are predominant throughout the year. The distribution of rainfall in the tropical zone of South America cannot be explained only by the migration of the ITCZ and the incidence of the trade winds; there are complex climatic patterns (Poveda & Mesa 1999). Different macroclimatic oscillations have been reported as sources of tropical variability close to the Colombian Caribbean coast: El Niño-South Oscillation (ENSO) has a strong influence on the hydrological cycle (Poveda et al. 2002, Poveda 2004), and the Madden-Julian Oscillation (MJO) and the Pacific Decadal Oscillation (PDO) also have some influence on the climate in this region (Jury 2017, Torres-Pineda & Pabón-Caicedo 2017, Garavito-Mahecha 2021). An increase in the magnitude of trade winds in the Caribbean during the winter is associated with the increase in the North Atlantic Subtropical High (NASH); this increase is enhanced during the positive phase of the North Atlantic Oscillation (NAO) (Van Loon & Rogers 1981, Giannini et al. 2001) where the heavy winds cause an appreciable rise in the significant wave height regime (Morales-Márquez et al. 2023).

Concerning Cfs, their effects are especially concentrated in the alteration of the sea state, mainly along the central and southwestern parts of Colombia's coastline; these effects generate extreme waves and cause severe damage to coastal infrastructure (Ortiz et al. 2014) and even affect the fishing activity in the area (Doria-González et al. 2022).

The historic pier of Puerto Colombia, in the Colombian Caribbean Sea, was destroyed by heavy waves in 2009 due to the arrival of a Cf on the morning of March 07 (Ortiz et al. 2014, Instituto Meteorológico Nacional de Costa Rica-IMN 2009). In addition to this, the strong waves generate flooding, causing economic damage to the communities that rely on fishing and tourism on the beaches for their livelihood. Concerning the extremely significant wave height regime, it has been determined that the central and southwestern 1,600 km of the Colombian coastline is dominated by the arrival of Cfs rather than the passing of tropical storms and hurricanes (Ortiz et al. 2014, Otero et al. 2016, Morales-Márquez et al. 2023). Other studies have determined that the increase in Cfs played a significant

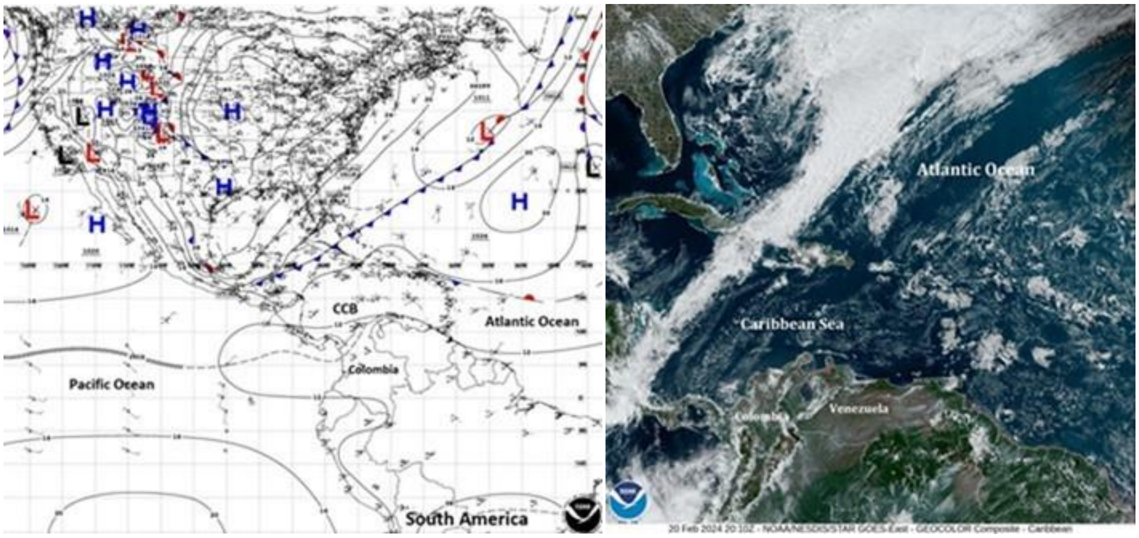

Figure 1. Arrival of a cold front on February 20, 2024, at 20:10Z. Left: modified from CIRA/NOAA GEOCOLOR imagery. Right: National Hurricane Center NHC/tropical analysis forecast branch of NOAA.

role in the so-called "Black summer" in Australia in 2019-2020, favoring atmospheric instability and becoming an important synoptic-scale driver of forest fire risk in this area of the Southern Hemisphere (Cai et al. 2022).

Studies reported in the literature demonstrate how the intrusion of fronts in the Caribbean leads to changes in regional weather patterns and their relationship with macroclimatic oscillations. For example, in the case of cold pushes, they tend to project from the polar sector towards the extratropical region and can reach the tropical zone. The advance of the anticyclone associated with the cold push to the south generates a strong pressure gradient between the extratropical and tropical flows. This gradient favors wind flow advancing southward over Central America and the Caribbean Sea, which interacts with the wind flow. In some cases, during its advance through the Central American sector and its maritime zone, the Cf may lag behind the shear line; this occurs from November to February. Occasionally, extra-temporal cold pushes occur, as happened in 2016 when a cold push entered Central America between May 5 and 9. However, these are infrequent and of weak intensity due to the decrease in thermal gradients between the Northern and Southern Hemispheres. It was found that the high number of cases presents greater negative temperature anomalies located to the north of Costa Rica, favoring a high thermal gradient between the cold and warm flows. In low-pressure cases, when cold temperature anomalies move towards the central part of the Caribbean Sea, this gradient is smaller, resulting in a lower response to extreme rainfall events. For the high cases, the wind showed greater magnitude and northern direction in the western Caribbean compared to the low cases. It was found that the westerly anomalies for the low cases invade much of the western Atlantic, suggesting less low-level convergence in southern Central America and within the Caribbean Sea. When synoptic configurations, such as those described above for the high cases, are identified, relevant extreme rainfall events may occur in the Caribbean and the northern zone of South America, as well as in the east and north of the Central Valley (Chinchilla et al. 2016, 2017). Their correlation with different sources of climate variability has been analyzed in some regions. For example, in the southern USA, a non-significant incidence of ENSO was established, along with an increase in the frequency of Cfs. In contrast, a stronger correlation was found between the NOA and the Pacific North American Oscillation. The Mexican climate is influenced by mid-latitude cyclones, which generate Cfs. Mid-latitude systems utilize this current system in the jet stream to acquire energy. The passage of Cfs in the north of the Mexican Republic has become more frequent, and with it, there have been more winter rains in the north and center of the country, as well as in the Yucatan Peninsula. The abnormally persistent presence of Cfs during El Niño winters causes temperatures in much of the country to be below normal, with snowfall in the Sierra Madre and even in the central part of Mexico (Magaña-Rueda et al. 1999, González 1999, Hardy & Henderson 2003, Lagerquist et al. 2020). Between 1923-1924 and 1995-1996, a direct positive relationship existed between Cfs and their penetration into the western region of Cuba during El Niño years (Hernández 2002). Additionally, the winter season in Cuba is framed within the so-called dry period, which lasts from November to April. During that season, weather systems such as extratropical lows, "sures" winds, and Cfs occurs, which affect the Cuban archipelago, mainly its western region, causing abrupt changes in the associated meteorological variables. These changes can sometimes present severe weather (González 1999). The passage of episodic Cfs northwest of the Gulf of Mexico generally induces the reversing of long-shelf flows down the south of Texas (Romero-Arteaga et al. 2022). However, there are no studies on the atmospheric teleconnection of Cfs along the Colombian Caribbean Sea coast. On the other hand, some studies suggest that the Quasi-Biennial Oscillation (QBO) also influences tropical climate variability (Gray et al. 2018, García-Franco et al. 2022).

In this sense, one of the main objectives of this study is to present the climatological characteristics, long-term trends, and large-scale teleconnections of Cfs in the Colombian Caribbean from 1996 to 2021. By employing statistical analyses and case studies, we aim to identify significant variations in Cfs occurrences and assess their relationship with major climate oscillations, including NAO, Pacific North American (PNA), QBO, and ENSO. Furthermore, this work seeks to enhance the understanding of how these climate patterns influence Cf activity, providing valuable information for improving weather forecasting and coastal risk management strategies.

This paper is structured as follows: Introduction, Methodology, Results (including statistical analyses and atmospheric teleconnection), Discussion, and the Conclusions

METHODOLOGY

Data

The information on the number of Cfs was obtained from the Centro de Investigaciones Oceanográficas e Hidrográficas Del Caribe Colombiano (CIOH 2022) for the period from 1996 to 2022. Monthly reports describe the various ocean-atmosphere interaction processes present in the Caribbean Sea and their primary characteristics. The CIOH of Colombia bases its meteomarine bulletins on information from several sources, including: numerical forecasting models which use global and regional atmospheric and oceanographic models, such as the Global Forecast System (GFS) and WaveWatch III (WW3) to predict waves, wind, currents and sea level: satellite images which receive data from meteorological and oceanographic satellites that allow them to monitor Cfs, tropical cyclones and other meteorological systems that affect the Caribbean Sea and the Colombian Pacific; oceanographic buoys and tide gauges which are equipment deployed at sea that measures variables such as temperature, pressure, wave height and sea level in real time; coastal meteorological stations which gathers data from stations installed at different points along the Colombian coast to monitor winds, rainfall and atmospheric pressure; and, finally, information from other international agencies such as reports from the National Oceanic and Atmospheric Administration (NOAA), the Instituto Hidrográfico de la Marina of Spain, and other meteorological and oceanographic centers. With this information, the CIOH generates daily bulletins and special bulletins when extreme phenomena occur, such as hurricanes or rough seas, which are crucial for navigation, fishing, and safety on the Colombian coasts (CIOH 2022).

For ENSO events, two main indices can be analyzed: the Southern Oscillation Index (SOI) and the Oceanic Niño Index (ONI): the SOI index indicates the development and intensity of El Niño (negative values) or La Niña events (positive values) in the Pacific Ocean, calculated using the pressure differences between Tahiti and Darwin, while the ONI index warm (positive values or El Niño) and cold (negative values or La Niña) periods are based on a threshold of ±0.5°C for the ONI [3-month running mean of ERSST.v5 SST anomalies in the Niño 3.4 region (5ºN-5ºS, 120-170ºW)] based on centered 30-year base periods updated every 5 years. Both indices were obtained from NOAA-Climate.gov (2024) for the period from 1996 to 2021. In this study, the index chosen is the SOI index.

The NAO index is based on the surface sea-level pressure difference between the Subtropical (Azores) High and the Subpolar Low. The time series was obtained from the National Centers for Environmental Information of the NOAA for the period from 1996 to 2021 (NCEI 2023). The PNA index was obtained from the National Weather Service Climate Prediction Center of NOAA. The monthly mean PNA index is constructed by projecting the (00Z) 500 mb height anomalies over the Northern Hemisphere onto the loading pattern of the PNA (Climate Prediction Center-NOAA 2023). In the case of the QBO index, it is calculated from the zonal average of the 30 mb zonal wind at the equator as computed from the National

Centers for Environmental Prediction (NCEP)/ National Center for Atmospheric Research (NCAR) reanalysis. The time series was obtained from the NOAA Physical Sciences Laboratory (NOAA-PSL 2024) for the period from 1996 to 2021.

Statistical analysis

For the statistical analysis, descriptive calculations were performed, including measures of central tendency, dispersion, and asymmetry. Histograms, box-and-whisker plots, and time series plots were developed to visualize trends, seasonality, and changes in the data over time. To analyze trends in the time series, we applied the Dickey-Fuller test which tests the null hypothesis (H_0) that the series has a unit root, i.e. it is non-stationary, against the alternative hypothesis (H_1) that the series is stationary. A *P*-value greater than 0.05 indicates that we do not reject the H_0, suggesting that the series is non-stationary. In such cases, the presence of a deterministic trend may be further assessed through regression analysis and moving averages. To further investigate the presence of a deterministic trend in the CFs time series, the following techniques were applied: moving average plots, linear regression analysis, and modeling time as an explanatory variable to predict the behavior of CFs over the study period. A low *P*-value would indicate evidence of a significant linear trend. The Mann-Kendall test (Mann 1945, Kendall 1975) was used to evaluate the presence of a monotonic trend in the total number of Cfs time series. Suppose the *P*-value is less than the significance level of 0.05. In that case, the H_0 of the absence of a monotonic trend can be rejected, which indicates that there is sufficient evidence to affirm that a trend exists in the time series. Finally, a correlation analysis was performed to evaluate the relationship between pairs of variables by calculating Spearman's correlation coefficient and visually representing the correlations through scatter plots or correlation matrices. A *P*-value greater than 0.05 indicates no association between the variables in question. A comparison of the number of Cfs concerning the different phases of macroclimatic oscillations was carried out. Strong positive and negative phases of the oscillations were defined as index values above or below the mean of each series during the Cf season in the study area (November to April).

Additionally, to assess whether the differences in Cf frequencies between the positive and negative phases of each oscillation were statistically significant, a Chi-square test for independence was applied. This test enabled us to assess the relationship between the oscillation phase and the number of Cfs observed, and the results are presented (Table 4). A *P*-value less than 0.05 was considered statistically significant.

Although advanced modeling techniques such as Generalized Linear Models (GLM) can offer additional inferential power, the present study is exploratory and based on a relatively short time series (n = 26 years), which limits the applicability of more complex parametric models without risking overfitting. Given this limitation, we prioritized robust, nonparametric methods and simple linear models that are suitable for small samples and allow for transparent interpretation of results. Moreover, we enhanced methodological rigor by detailing the data acquisition and quality control procedures. Meteorological and climatic indices were collected from official sources (CIOH, NOAA), and quality assurance included cross-validation with multiple databases, consistency checks, and appropriate handling of missing or anomalous values. This methodological framework ensures a reliable basis for evaluating long-term variability in cold front activity and its potential relationships with large-scale climate oscillations.

RESULTS

Climatology of cold fronts (Cfs)

Table 1 shows the frequency of Cfs arriving on the Colombian Caribbean Sea coast. They arrive as early as November and some as late as April, which both average 30 CFs, but the peak of frequency is in January with 52 CFs (Fig. 2).

Two hundred thirty-three Cfs have arrived at the Caribbean Sea during the study period, with the highest frequency being in 2019 (29) and the lowest frequency of occurrence being 3 in 1997, 2001, and 2004.

Table 2 presents various statistical measures for the values corresponding to the number of Cfs during the period from 1996 to 2021. The mean values in Table 2 indicate that the region experienced, on average, 9 Cfs during that time. The corresponding distributions are skewed to the right, as observed from the minimum, maximum, and coefficient of variation (CV) values of the dataset. Analyzing the 75th and 25th percentiles, it is observed that, in Colombia, 75% of the number of Cfs is greater than or equal to 13, and this occurs during the months with the highest frequency. On the other hand, during the months of lower frequency, 25% of the Cfs are less than or equal to 5.

Table 1. Statistical measures of cold front passage frequencies during the period from 1996 to 2021 in the Colombian Caribbean Sea coast. The year value is for the two values: November-December and January-April.

Year	Nov	Dec	Jan	Feb	Mar	Apr	Total	Mean
1996	1	0	1	1	1	1	5	0.83
1997	1	1	1	0	0	0	3	0.50
1998	1	0	1	1	1	1	5	0.83
1999	0	1	1	2	2	1	7	1.17
2000	0	1	1	2	0	1	5	0.83
2001	0	1	0	0	1	1	3	0.50
2002	0	1	1	1	1	1	5	0.83
2003	0	0	2	1	0	1	4	0.67
2004	0	1	0	1	0	1	3	0.50
2005	2	1	1	2	2	1	9	1.50
2006	1	1	0	0	2	1	5	0.83
2007	2	1	2	2	1	2	10	1.67
2008	1	1	2	1	1	2	8	1.33
2009	1	1	1	1	1	1	6	1.00
2010	1	1	1	1	1	1	6	1.00
2011	1	1	1	1	1	0	5	0.83
2012	0	0	1	1	1	1	4	0.67
2013	3	2	2	2	3	1	13	2.17
2014	3	3	5	2	4	2	19	3.17
2015	0	5	3	4	1	0	13	2.17
2016	1	1	5	4	2	3	16	2.67
2017	0	1	5	3	3	2	14	2.33
2018	3	6	4	0	4	1	18	3.00
2019	7	7	7	2	3	3	29	4.83
2020	0	4	2	3	2	1	12	2.00
2021	1	2	2	1	0	0	6	1.00
Total	30	44	52	39	38	30	233	
Mean	1.15	1.69	2.00	1.50	1.46	1.15	8.96	

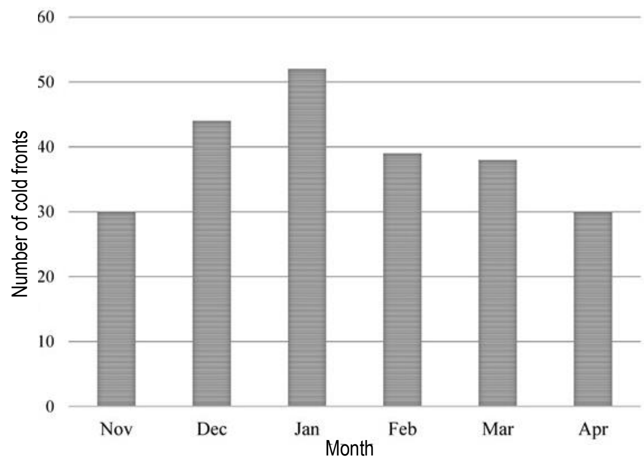

Figure 2. Seasonal variation of the number of cold fronts in the Caribbean Sea. The bars represent the total occurrences from 1996-2021.

Table 2. Statistical measures for the values corresponding to the total number of cold fronts (Cfs) during the period from 1996 to 2021. CV: coefficient of variation, Q1: first quartile (25th percentile), Median: 50th percentile, Q3: third quartile (75th percentile). SD: standard deviation.

Measure	CF total
Min	3.00
Max	29.00
Mean	8.96
SD	6.27
CV	70%
Skewness	1.42
Q1	5.00
Median	6.00
Q3	13.00

For the Cfs time series, a linear pattern is observed during the period from 1996 to 2012, with values ranging between 3 and 10 Cfs and an average of approximately 5.47. Then, from 2013 to 2019, the trajectory ascends, with values oscillating between 13 and 29 Cfs, or an average of approximately 17.43 Cfs. Finally, in 2020 and 2021, the values decrease (12 and 6, respectively).

The results obtained from the Dickey-Fuller test (ADF = -2.3284, *P*-value = 0.4473) indicate that the H_o of a unit root cannot be rejected (*P*-value > 0.05), suggesting that the CF_total time series is non-stationary. This non-stationarity may be associated with the presence of a deterministic trend. Such a trend can be observed intuitively (Fig. 3), which displays the CF_total time series (dots) along with a solid line representing the 2-year moving average, calculated by averaging every two consecutive annual values. This visualization helps to highlight short-term fluctuations and the overall upward pattern observed during the latter part of the period.

The results found by performing a linear regression test (F-statistic = 19.39 on 1 and 24 degrees of freedom, *P*-value = 0.0002) indicate strong evidence of a significant linear trend in the CF_total time series over time (*P*-value < 0.05). Since the slope of the time variable is statistically significant, this confirms the existence of a positive linear relationship between time and the number of Cfs. Complementing the above, the results of the Mann-Kendall test (Z = 3.4926, n = 26, *P*-value = 0.0048) also indicate a significant monotonic trend in the series. Together, these findings provide consistent evidence of an increasing trend in Cf frequency over the study period.

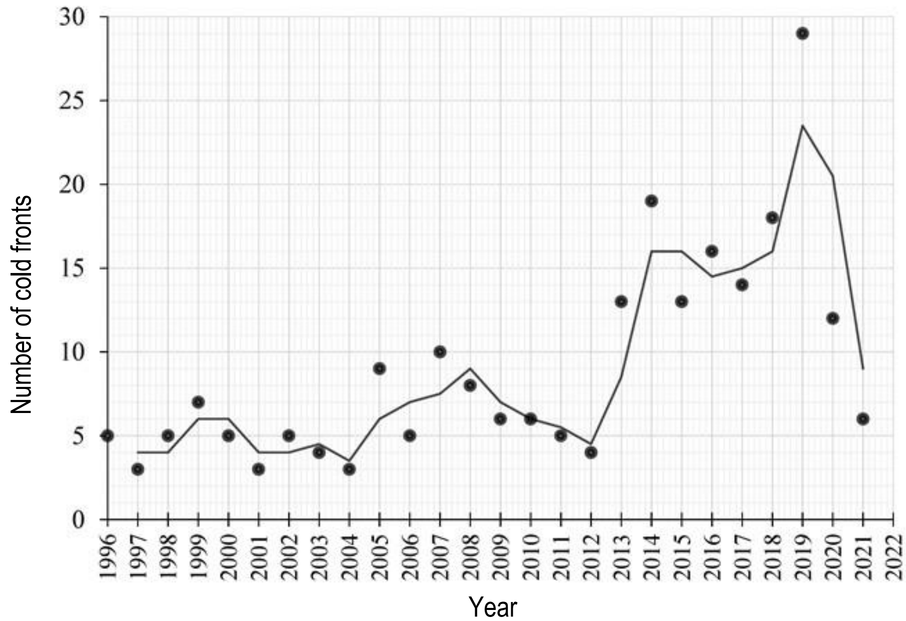

Figure 3. Cold fronts (Cfs) CF_total time series from 1996 to 2021. Annual values are shown as black dots, and the solid line represents a 2-year moving average used to highlight short-term trends.

Statistical analysis of macroclimatic indexes

Most of the results presented above, especially those related to variability, are shown (Fig. 4), which represents the box-and-whisker plots of the mean NAO, PNA, QBO, and SOI indices distributed by intervals that aggregate the range of values of the number of Cfs.

Figure 5 shows the distribution of the values corresponding to the number of CF_total and the averages of the NAO, PNA, QBO, and SOI indices. In the case of CF_total, it is observed that in that time interval, between 3 and 29 Cfs occurred in Colombia. In particular, 5 Cfs occurred 6 times, but from this graph, we cannot find the specific time interval(s) in which they occurred. For the rest of the number of Cfs (3 to 4 and 6 to 29), the frequency of occurrences oscillates between 1 and 3. For the case of the mean NAO index values (NAO_mean), some peaks are observed, which oscillate between -0.5 and 0.5. In the case of the mean PNA (PNA_mean) indices, the peaks range between 0 and 0.4; and, for the mean SOI (SOI_mean), these mean values are around -3 and 3, approximately, and for the mean QBO (QBO_mean), the values range from -20 to 11.

While these histograms do not provide temporal resolution (i.e. they do not show when specific values occurred), they are useful for summarizing the distributional characteristics, data dispersion, and central tendencies of the variables included in the analysis. These graphical summaries help confirm the asymmetry, range, and frequency patterns, which are crucial in interpreting correlation results and selecting the appropriate statistical tests for the next stages of analysis.

Spearman correlation and atmospheric teleconnection

Table 3 presents the results of the Spearman correlation analysis between the total number of Cfs CF_total and the mean values of the NAO, PNA, QBO, and SOI during the Cf season (November-April) over the period from 1996-2021. The table displays the Spearman correlation coefficient (ρ) and its corresponding *P*-value, which indicate the strength and statistical significance of the monotonic relationship between the variables.

According to the results, none of the correlations are statistically significant at the 5% level ($P > 0.05$), suggesting that the associations observed may be weak or due to chance. The SOI shows a negligible relationship with CF_total ($\rho = 0.04$, $P = 0.83$), while QBO ($\rho = 0.17$, $P = 0.41$) and NAO ($\rho = 0.25$, $P = 0.23$) show weak positive but non-significant correlations. The strongest (though still not statistically significant) correlation was found with the PNA index ($\rho = 0.31$, $P = 0.12$), which may suggest a moderate relationship worthy of further investigation with larger datasets. These findings highlight the complexity of the climatic

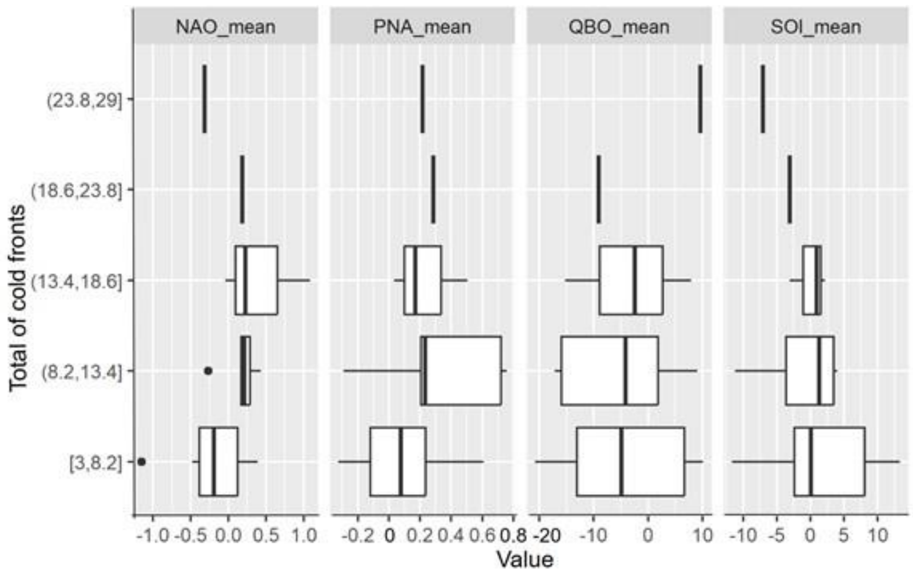

Figure 4. Values corresponding to the mean values (November-April) of the North Atlantic Oscillation (NAO), Pacific North American (PNA), Quasi-Biennial Oscillation (QBO), and Southern Oscillation Index (SOI), according to total of cold fronts (Cfs), and the period 1996-2021 of total of Cfs.

Table 3. Spearman correlation coefficients (rho) and *P*-value of the correlation test (*p*) between the mean of North Atlantic Oscillation (NAO), Pacific North American (PNA), Quasi-Biennial Oscillation (QBO), and Southern Oscillation Index (SOI) indices and cold fronts passage frequencies during the period from 1996 to 2021.

Index	rho	*P*-value
NAO	0.25	0.23
PNA	0.31	0.12
QBO	0.17	0.41
SOI	0.04	0.83

interactions and the limited influence of individual indices in explaining Cf variability at low latitudes. Table 3 summarizes the Spearman correlation coefficients and their corresponding *P*-values.

Additionally, Figure 6 provides a visual representation of the same results through a color-coded correlation matrix, where the strength and direction of each correlation are depicted using a blue-red scale. A red "X" has been added to the cells where the correlation is not statistically significant ($P > 0.05$), helping the reader quickly identify relationships that may not be meaningful.

Although none of the individual correlations reached statistical significance ($P > 0.05$), the positive association with the PNA index suggests a possible climatological influence that warrants further exploration with expanded datasets and multivariate modeling techniques.

Another analysis involved establishing a comparison between the number of Cfs and the opposite phases of each oscillation, as the Spearman correlation process does not reveal the connection between the different phases of the oscillations and the number of Cfs (Hardy & Henderson 2003).

To establish a strong positive and negative, the mean of the absolute values of each index was used. The following were assessed in the case of ENSO, where Cf passage frequencies during months having a positive index value (index values ≥ 0.5, El Niño) were compared to Cf passage frequencies during months having a negative index value (index values ≤ -0.5, La Niña). The other index values were compared with the QBO index values being ≥ 6.2 and ≤ -6.2; the NAO index values being ≥ 0.5 and ≤ -0.5, and the PNA index values being ≥ 0.3 and ≤ -0.3 respectively.

Table 4 indicates the comparison of Cf passage frequencies during the opposite phases of each teleconnection, with Cfs being much more frequent in the positive phase of ENSO. These results are consistent with the work of Hernández (2002) in Cuba, as well as in the states of New Mexico, Texas, Oklahoma, Arkansas, Louisiana, Mississippi, Alabama, Georgia, and South Carolina, according to Hardy & Henderson (2003).

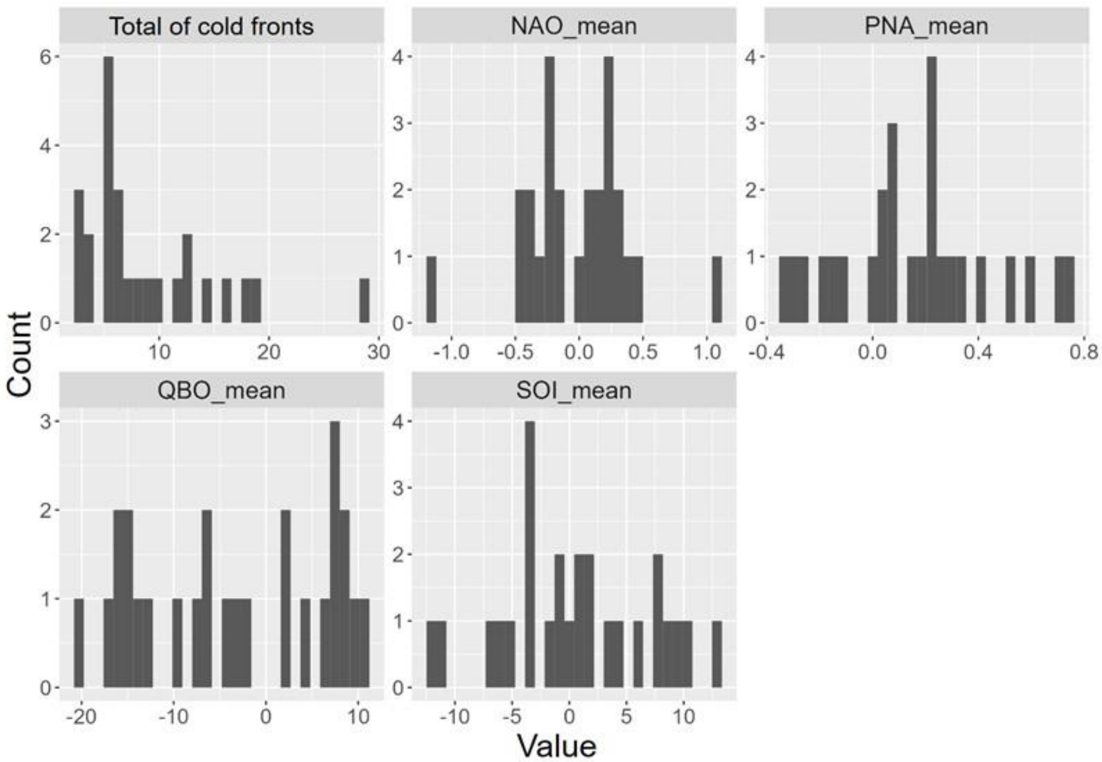

Figure 5. Distribution of the values corresponding to the Cf_total and the averages (November-April) of the North Atlantic Oscillation (NAO), Pacific North American (PNA), Quasi-Biennial Oscillation (QBO), and Southern Oscillation Index (SOI) indices during the period from 1996 to 2021.

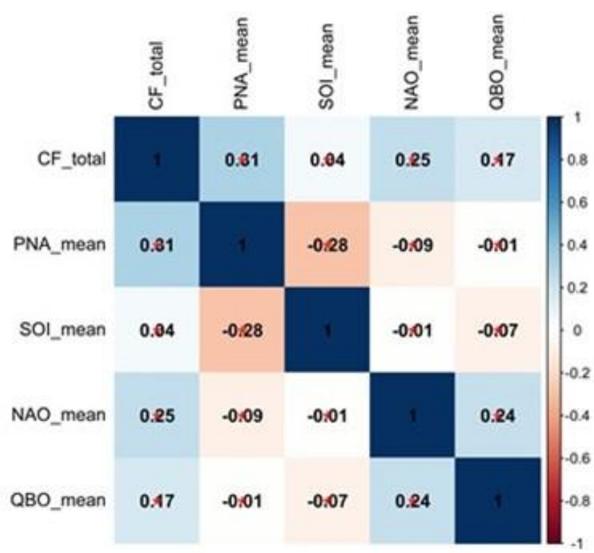

Figure 6. Spearman correlation matrix between cold front frequency (CF_total) and mean values of macroclimatic indices (North Atlantic Oscillation (NAO), Pacific North American (PNA), Quasi-Biennial Oscillation (QBO), and Southern Oscillation Index (SOI)) during the cold front season (November-April), from 1996 to 2021. Blue indicates positive correlations, red indicates negative correlations, and the color intensity reflects the strength of the association. A red "X" marks non-significant correlations ($P > 0.05$).

Table 4. Total number of cold fronts (Cfs) observed during strong positive and negative phases of each macroclimatic oscillation, with results of the Chi-square test of independence (χ^2) and associated *P*-values. Bold values indicate statistically significant differences ($P < 0.05$). The data correspond to the Cf seasons from 1996 to 2021 (November-April).

Oscillation	Positive (+)	Negative (-)
ENSO	54	34
QBO	28	72
NAO	133	6
PNA	60	18

To assess whether these differences were statistically significant, a Chi-square test for independence was applied to each pair of phases. The results indicate that the differences are statistically significant ($P < 0.05$) in the cases of NAO, PNA, and QBO, while for ENSO, the difference was not significant ($P = 0.1063$), suggesting that although more Cfs occur during El Niño, the relationship is not strong enough to be statistically conclusive.

Figure 7a shows that the number of Cfs in both the positive (54) and negative (34) phases of ENSO is similar, although there is a slight difference in the increase of Cfs during the El Niño phase. Figure 7b shows that the largest number of fronts (72) occurs during the negative phase of QBO. The likely effect of the QBO on the Cf is unclear.

The situation is different with NAO; these results are consistent with all Cfs arriving in all states analyzed by Hardy & Henderson (2003) in the southern USA. The marked difference between the number of Cfs during the positive phase of the NAO is explained by the fact that the greatest number of fronts (121) occurred between 2014 and 2020, corresponding to NAO positive indices values (Fig. 7c). The numbers of Cfs (67) during the positive phase of the PNA occurred between 1997 and 2016, corresponding to positive indices close to a 0.5 index value (Fig. 7d). One of the events examined in this study was analyzed in detail. The development of the baroclinic cyclone and the advancement of the frontal system towards the Colombian Caribbean Coast occurred between January 9 and 11, 2021 (Instituto Meteorologico Nacional de Costa Rica-IMN 2021), where it is possible to observe its strengthening over the hours (Fig. 8). Its core was observed only at low levels of the atmosphere, while at medium and high levels only the intense westward flow was identified, with the presence of the Subtropical Jet Stream. The core remained fixed at approximately latitude 35°N, with a northeastward displacement, presenting closed isobars around 994 mbar, according to Mean Sea Level Pressure (MSLP) data. In the early hours of January 9, the advancement of cold air can be observed across the temperature advection fields over parts of the Caribbean and Central America (12 UTC, Fig. 8a). This exhibited quite visible baroclinic characteristics, with cold advection at the forefront of the system and warm advection at the rear. The position of the frontal system also stood out in terms of geopotential, with the Cf's progress following the propagation of cold air along the trough axis, reaching the study area with greater intensity at 00 UTC on January 10 (Fig. 8b). The increased intensity of convection associated with the frontal system in the Colombian Caribbean region began several hours after the frontal system entered the area, encountering the warm air mass present in the region (06 UTC, Fig. 8c). At the same time, satellite images indicate the development of convective cells with intense vertical growth, with cloud top temperatures ranging between -60 to -70°C (Fig. 8g).

The weakening of the frontal edge occurred gradually throughout the hours of January 10, with the dissipation of cloudiness associated with the system occurring around 20 UTC, where the frontal system's characteristics could no longer be observed in the meteorological fields (Fig. 7d) or satellite images (Fig. 7h).

DISCUSSION

Regarding global warming, some studies suggest that as global temperatures rise, cold fronts are expected to decrease (Seneviratne et al. 2021). However, in a large part of the USA, the intensity of Cfs does not appear to be decreasing at the same rate due to variability in the polar vortex associated with Arctic warming (Cohen et al. 2021). In this study (1996-2021), there is evidence of an increase of 6 to 9 Cfs per year, compared to the last study (1996-2012) by Ortiz et al. (2013). In addition to finding that January is the month where most Cfs arrive (2 on average), it is observed that in that time interval, between 3 and 29 Cfs occurred in the Caribbean Sea. The Dickey-Fuller test indicates that the Cf series is not stationary. Additionally, a linear regression test, along with Kendall's test, provides sufficient evidence to affirm the presence of a trend in the time series.

This study reveals that none of the macroclimatic oscillations analyzed had a significant impact on the

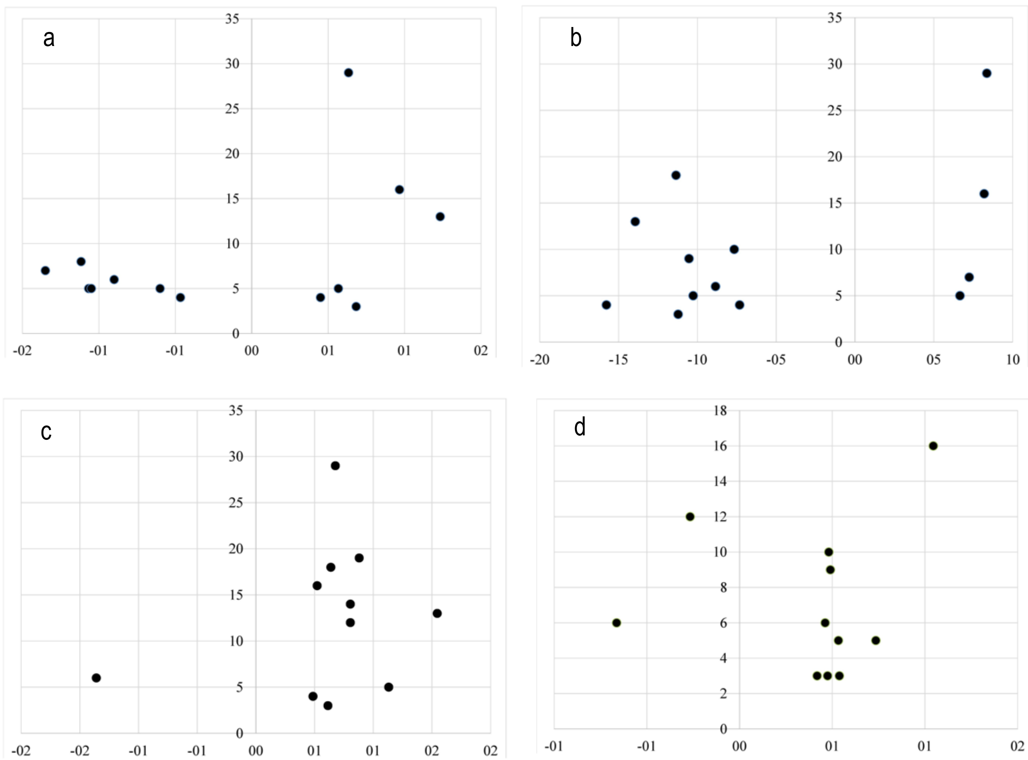

Figure 7. Comparison of the number cold front passage frequencies during the strong opposite phases (positive and negative indexes values in the x axis) of each teleconnection pattern during the period 1996-2021: a) El Niño-Southern Oscillation, ENSO (mean value 0.5), b) Quasi-Biennial Oscillation, QBO (mean value 6.2), c) North Atlantic Oscillation, NAO (mean value 0.5) and d) Pacific North American (PNA) (mean value 0.3).

arrival of Cfs at low latitudes during the period from 1996 to 2021. Of all of them, the NAO positive phase could have the greatest effect. In this regard, it coincides with the fronts in the southern USA, which also aligns with Zárate-Hernández (2013) using the NAO-AO relationship. Strongly positive phases of the NAO are usually associated with above-average temperatures in the eastern USA and northern Europe and below-average temperatures in Greenland and often in southern Europe and the Middle East (Hardy & Henderson 2003). Local effects, such as the currents of the North Atlantic Ocean, can influence the displacement of fronts to lower latitudes. These currents can affect the temperature distribution in the overlying atmosphere. Areas of warmer waters tend to heat the air above them, increasing instability that can intensify temperature gradients and, consequently, promote the further advancement of Cfs. According to Hardy & Henderson (2003), the increase of Cf activity during the El Niño winter may be related to the strengthened upper-air westerlies over the Gulf of Mexico affecting the frequency of Cfs over the Caribbean Sea. In addition, the positive phase of the PNA pattern is associated with above-average temperatures in western Canada and the far western USA and below-average temperatures in the south-central and southeastern USA, and these low temperatures probably favor the transit of Cfs to the Caribbean Sea, consistent with a similar study by Zárate-Hernández (2014).

On the other hand, Walker's circulation is weaker during QBO westerly (QBOW or positive index values) compared to QBO easterly (QBOE or negative index values). During El Niño events, in addition to QBOW, subtropical jets, and the polar vortex become stronger, so a possible relationship between El Niño and QBO has also been investigated (García-Franco et al. 2022, Kumar et al. 2022, Labe et al. 2019).

The January 2021 case study revealed the development and progression of a baroclinic cyclone and its associated frontal system towards the Colombian Caribbean Sea. The detailed analysis of the event between January 9 and 11, 2021, revealed that the system's core remained at low atmospheric levels, characterized by intense westward flow and the presen-

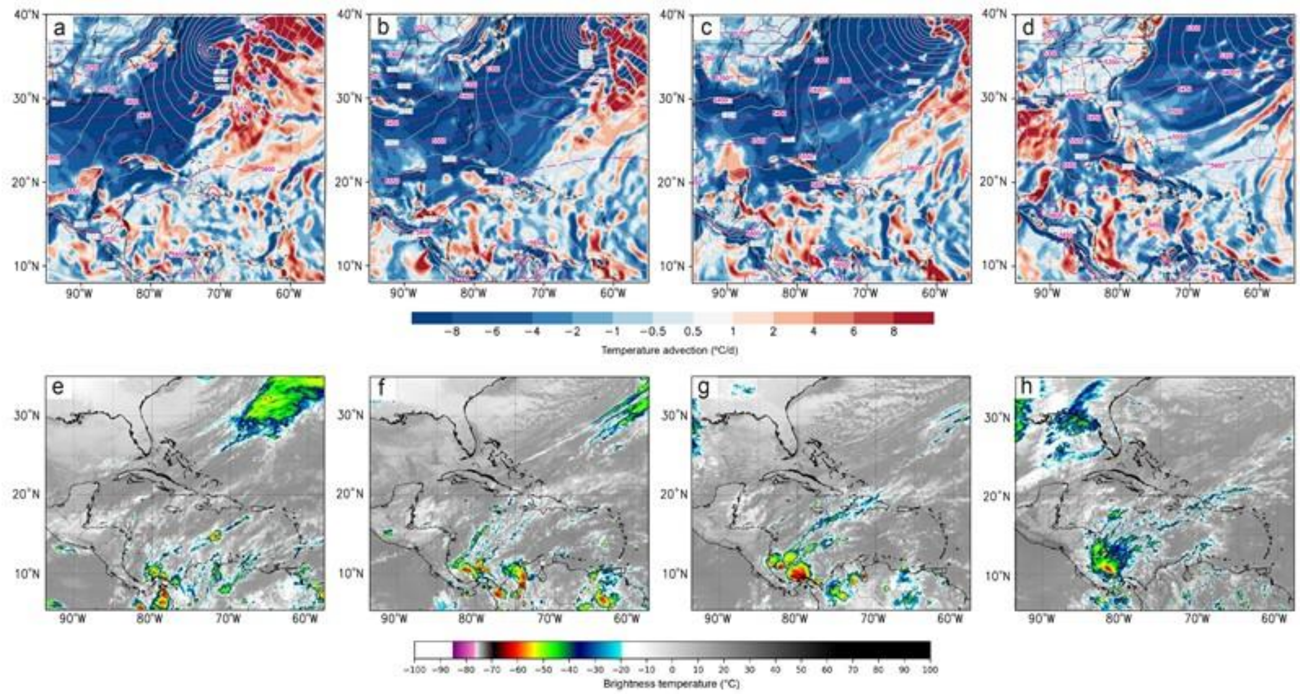

Figure 8. Temperature advection (°C d^{-1}; shaded; 1,000 mb), sea level pressure (mb, gray contour), and geopotential height (mgp; pink shaded contour; 1,000-500 mb) on a) January 09: 12 UTC, b) January 10: 00 UTC, c) January 10: 06 UTC, and d) January 10: 20 UTC; GOES-16 satellite images in the infrared channel (channel 13; 10.3 μm) on e) January 09: 12 UTC, f) January 10: 00 UTC, g) January 10: 06 UTC and h) January 10: 20 UTC.

ce of the Subtropical Jet Stream at higher levels. The Cf's advance brought visible baroclinic characteristics, with distinct cold and warm air advection. The system's impact peaked on January 10, marked by significant convection and the formation of convective cells, as observed in satellite imagery. The frontal system gradually weakened and dissipated by the evening of January 10, losing its distinct meteorological characteristics.

Although some advanced statistical models, such as GLM, could enhance the understanding of complex relationships among variables such as temperature, wind, and Cf frequency, their application requires specific conditions (e.g. large sample size and certain distributional assumptions) that are not met by this study's relatively short time series (n = 26). In this exploratory context, simpler statistical techniques such as trend analysis (Dickey-Fuller, Mann-Kendall), linear regression, and Spearman correlations were deemed more appropriate and robust for the available data. These methods enabled an effective preliminary assessment of long-term behavior while minimizing the risk of overfitting and maintaining transparency in the interpretation of results.

Furthermore, the statistical comparison of Cf frequencies during the strong positive and negative phases of each oscillation using the Chi-square test showed significant differences in the cases of NAO, QBO, and PNA ($P < 0.05$), reinforcing the potential influence of these oscillations in modulating Cf activity at tropical latitudes.

CONCLUSIONS

This study presents a detailed climatological analysis of Cfs affecting the Colombian Caribbean Sea from 1996 to 2021, with an emphasis on their frequency, long-term trends, and association with large-scale atmospheric teleconnection patterns. The results demonstrate a significant increase in Cf occurrences compared to previous assessments, with 6 to 9 additional events per year. This trend was supported by robust statistical evidence, including the Augmented Dickey-Fuller and Mann-Kendall tests, which confirmed the non-stationary and monotonic nature of the time series.

The seasonal distribution revealed that January is the month with the highest frequency of Cfs, consistent with enhanced baroclinic activity and stronger meridional thermal gradients during the boreal winter. A total of 233 events were documented over the study period, with 2019 showing the highest number of occurrences. These findings suggest that contrary to some expectations regarding global warming and a potential reduction in cold air outbreaks at tropical latitudes, Cfs continue to exert an increasingly important influence on the region's atmospheric dynamics, which may be associated with the influence of Arctic amplification and its effects on mid-latitude circulation patterns, including the polar vortex.

The analysis of atmospheric teleconnection patterns showed that while ENSO and QBO presented weak or statistically insignificant relationships with Cf frequencies, the NAO and the PNA pattern exhibited stronger associations. In particular, the positive phases of NAO and PNA were significantly linked to increased Cf activity, as confirmed by the Chi-square test. These findings are in agreement with previous studies conducted in the southeastern USA and Central America, suggesting that these mid-latitude modes play a relevant role in modulating frontal incursions into the Caribbean.

The case study of the January 2021 event allowed for a detailed assessment of the synoptic evolution of a baroclinic system. The event was characterized by the development of a frontal system associated with strong cold advection and the presence of the Subtropical Jet Stream at upper levels, which contributed to the system's intensification. The progression of the frontal boundary across the Colombian Caribbean was accompanied by significant convection and intense atmospheric instability, illustrating the potential severity of such systems even at low latitudes.

This work contributes to filling an important gap in the literature by being the first to investigate the climatology, temporal evolution, and teleconnections of Cfs in the Colombian Caribbean Sea in detail, utilizing long-term observational data. The findings highlight the increasing significance of Cfs as a driver of hydro-meteorological extremes in the region, particularly about coastal vulnerability, maritime safety, and climate risk management.

Given the relatively short period of analysis (26 years), further studies should extend the dataset and include longer-period oscillations such as the Pacific Decadal Oscillation and the Atlantic Multidecadal Oscillation. Furthermore, future work should incorporate numerical modeling approaches to examine the underlying dynamics of Cf intensification within the context of a changing climate and its interactions with regional ocean-atmosphere processes.

Credit author contribution

J.C. Ortiz: conceptualization, validation, methodology, formal analysis, writing-. original draft; H. Llinás: supervision, review, and editing; H. Gomes: methodology, validation, supervision, review, and editing; M. Lyra: methodology, data curation, formal analysis, review, and editing. All authors have read and accepted the published version of the manuscript.

Conflict of interest

The authors declare no conflict of interest.

ACKNOWLEDGMENTS

The authors wish to thank Centro Colombiano de Datos Oceanográficos (CECOLDO) of the Centro de Investigaciones Oceanográficas e Hidrográficas del Caribe (CIOH) de la Dirección Marítima Nacional de Colombia (DIMAR) for providing the meteorological information and particularly the transit of cold fronts in the study area.

REFERENCES

Amador, J.A., Alfaro, E.J., Lizano, O.G., et al. 2006. Atmospheric forcing in the Eastern Tropical Pacific: A review. Progress in Oceanography, 69: 101-142. doi: 10.1016/j.Pocean.2006.03.007

Beringer, J. & Tepper, N.J. 2000. The influence of subtropical cold fronts on the surface energy balance of a semi-arid site. Journal of Arid Environmental, 44: 437-450. doi: 10.1006/jare.1999.0608

Cai, D., Abram, N.J., Sharples, J.J., et al. 2022. Increasing intensity and frequency of cold fronts contributed to Australia’s 2019-2020 Black Summer fire disaster. Environmental Research Letters, 17: 094044. doi: 10.1088/1748-9326/ac8e88

Centro de Investigaciones Oceanográficas e Hidrográficas del Caribe Colombiano (CIOH). 2022. CIOH, Cartagena. [https://cecoldodigital.dimar.mil.co/view/divisions/BMCC/]. Reviewed: January 10, 2022.

Chinchilla, G., Gutiérrez, J. & Zárate, E. 2016. Eventos extremos de lluvia ocasionados por empujes fríos que han llegado a Costa Rica en el periodo invernal (NDEF) del año 2000 al 2010: Líneas de cortante. Tópicos Meteorológicos y Oceanográficos, 15: 48-62.

Chinchilla, G., Gutiérrez, J. & Zárate, E. 2017. Análisis sinóptico de casos de eventos extremos de lluvia asociados a líneas de cortante de empujes fríos que han llegado a Costa Rica en el periodo invernal. Tópicos Meteorológicos y Oceanográficos, 16: 5-18.

Climate Prediction Center-NOAA 2023. NOAA, Washington D.C. [https://www.cpc.ncep.noaa.gov/products/precip/CWlink/pna/pna_index.html]. Reviewed: January 10, 2025.

Cohen, J., Agel, L., Barlow, M., et al. 2021. Linking Arctic variability and change with extreme winter weather in the United States. Science, 373: 1116-1121. doi: 10.1126/ science.abi9167

Doria-González, M.A., Pérez-Ferro, D., Olaya, F.C., et al. 2022. Climate variability and small-scale fisheries of the Albuquerque Cays Island, insular Colombian Caribbean. Latin American Journal of Aquatic Research, 50: 596-609. doi: 10.3856/vol50-issue4-fulltext-2915

Faustino-Eslava, D.V., Graciano, F., Yumul Jr., P., et al. 2011. The January 2009 anomalous precipitation associated with the "Tail-end of the Cold Front" weather system in northern and eastern Mindanao (Philippines), natural hazards, impacts and risk reductions. Global Planet Change, 76: 85-94. doi: 10.1016/j.gloplacha.2010.12.009

Garavito-Mahecha, J.D. 2021. Determinación de la relación entre la Oscilación Decadal del Pacífico y la activación del ciclo ENOS en estaciones costeras e insulares del Pacífico colombiano. Tesis de Maestría, Universidad Nacional de Colombia, Bogotá.

García-Franco, J.L., Gray, L.J., Osprey, S., et al. 2022. The tropical route of quasi-biennial oscillation (QBO) teleconnections in a climate model. Weather Climate Dynamics, 3: 825-844. doi: 10.5194/wcd-3-825-2022

Garreaud, R.D. 2001. Subtropical cold surges: regional aspects and global distribution. International Journal of Climatology, 21: 1181-1197. doi: 10.1002/joc.687

Giannini, A., Cane, M.A. & Kushnir, Y. 2001. Interdecadal changes in the ENSO teleconnection to the Caribbean region and the North Atlantic oscillation. Journal of Climate, 14: 2867-2879. doi: 10.1175/1520-0442(2001)014<2867:ICITET>2.0.CO;2

González, C. 1999. Climatología de frentes fríos que han afectado Cuba desde 1916-1917 hasta 1996-1997. Revista Cubana de Meteorología, 66: 15-19.

Gray, L.J., Anstey, J.A., Kawatani, Y., et al. 2018. Surface impacts of the Quasi Biennial Oscillation. Atmospheric Chemistry and Physics, 18: 8227-8247. doi: 10.5194/acp-18-8227-2018

Hardy, J.W. & Henderson, K.G. 2003. Cold front variability in the southern United States and the influence of atmospheric teleconnection patterns. Physical Geography, 24: 120-137. doi: 10.2747/0272-3646.24.2.120

Hernández, B. 2002. El Niño-Oscilación del Sur (ENOS) y los frentes fríos que arriban a la región occidental cubana. Investigaciones Marinas, 30: 3-19. doi: 10.4067/S0717-71782002000 200001

Instituto Meteorológico Nacional de Costa Rica-IMN. 2009. IMN, San José. [https://www.imn.ac.cr/documents/10179/14629/MARZO]. Reviewed: April 4, 2025.

Instituto Meteorológico Nacional de Costa Rica-IMN. 2021. IMN, San José. [https://www.imn.ac.cr/documents/10179/506403/ENERO]. Reviewed: April 4, 2025.

Instituto Meteorológico Nacional de Costa Rica-IMN. 2024. IMN, San José. [https://www.imn.ac.cr/documents/10179/588211/FEBRERO]. Reviewed: April 4, 2025.

Jury, M. 2017. MJO influence in the Caribbean. Theoretical and Applied Climatology, 139: 1559-1567. doi: 10.1007/s00704-019-03037-x

Kendall, M.G. 1975. Rank correlation methods. Charles Griffin, London.

Kumar, V., Yoden, S. & Hitchman, M.H. 2022. QBO and ENSO effects on the mean meridional circulation, polar vortex, subtropical westerly jets, and wave patterns during boreal winter. Journal of Geophysical Research: Atmospheres, 127: e2022JD036691. doi: 10.1029/2022J D036691

Labe, Z., Peings, Y. & Magnusdottir, G. 2019. The effect of QBO phase on the atmospheric response to projected Arctic Sea ice loss in early winter. Geophysical Research Letters, 46: 7663-7671. doi: 10.1029/2019GL083095

Lagerquist, K., Allen, J.T. & McGovern, A. 2020. Climatology and variability of warm and cold fronts over North America from 1979 to 2018. Journal of Climate, 33: 6531-6554. doi: 10.1175/JCLI-D-19-0680.1

Locatelli, J.D., Sienkiewicz, J.M. & Hobbs, P.V. 1989. Organization and structure of clouds and precipitation on the mid-Atlantic coast of the United States. Part I: Synoptic evolution of a frontal system from the Rockies to the Atlantic Coast. Journal Atmospheric Science, 46: 1327-1348. doi: 10.1175/1520-0469 (1989)046<1327:OASOCA>2.0.CO;2

Magaña-Rueda, V.O., Pérez, J.L., Vázquez, J.L., et al. 1999. El Niño y el clima. In: Magaña-Rueda, V.O. (Ed.). Los impactos de El Niño en México. El Niño y el clima. Centro de Ciencias de la Atmósfera, México D.F., pp. 23-66.

Mann, H.B. 1945. Nonparametric tests against trend. Econometrica, 13: 245-259. doi: 10.2307/1907187

Morales-Márquez, V., Cáceres-Euse, A., Hernández-Carrasco, I., et al. 2023. Extreme waves in the Caribbean Sea: spatial regionalization and long-term analysis. Frontiers in Marine Sciences, 10: 1294189. doi: 10.3389/fmars.2023.1294189

Narváez, G. & León, G. 2003. Intrusion of cold air in tropical areas. Case study from January 5 to January 8, 2002. Meteorología Colombiana, 7: 99-108.

National Center of Environmental Information (NCEI). 2023. [https://www.ncei.noaa.gov/access /monitoring/nao/]. Reviewed: January 10, 2023.

National Oceanic and Atmospheric Administration-Physical Sciences Laboratory (NOAA-PSL). 2024. [https://psl.noaa.gov/data/correlation/qbo.data]. Reviewed: January 22, 2024.

National Oceanic and Atmospheric Administration-Climate (NOAA-Climate.gov). 2024. [https://www.climate.gov/news-features/understanding-climate/climate-variability-southern-oscillation-index]. Reviewed: January 22, 2024.

Ortiz, J.C., Salcedo, B. & Otero, L.J. 2014. Investigating the collapse of the Puerto Colombia Pier (Colombian Caribbean Coast) in March of 2009: Methodology for the reconstruction of extreme events and their impact on the coastal infrastructure. Journal of Coastal Research, 30: 291-300. doi: 10.2112/JCOASTRES-D-12-00062.1

Ortiz, J.C., Otero, L.J., Restrepo, J.C., et al. 2013. Cold fronts in the Colombian Caribbean Sea and their relationship to extreme wave events. Natural Hazards and Earth System Sciences, 13: 2797-2804. doi: 10.5194/nhess-13-2797-2013

Otero, L., Ortiz, J.C., Ruiz-Merchan, J.K., et al. 2016. Storms or cold fronts: what is really responsible for the extreme waves regime in the Colombian Caribbean coastal region? Natural Hazards and Earth System Sciences, 16: 391-401. doi: 10.5194/nhess-16-391-2016

Poveda, G. 2004. La hidroclimatología de Colombia: una síntesis desde la escala inter-decadal hasta la escala diurna. Revista de la Academia Colombiana de Ciencias Exactas y Naturales, 28: 201-222. doi: 10.18257/raccefyn.28(107).2004.1991

Poveda, G. & Mesa, O. 1999. La Corriente de Chorro Superficial del Oeste ("del CHOCÓ") y otras dos corrrientes de chorro atmosféricas sobre Colombia: Climatología y variabilidad durante las fases del ENSO. Revista de la Academia Colombiana de Ciencias Exactas y Naturales, 23: 517-528. doi: 10.18257/raccefyn.23(89).1999.2848

Poveda, G., Vélez, J.I., Mesa, O., et al. 2002. Influencia de fenómenos macroclimáticos sobre el ciclo anual de la hidrología colombiana: cuantificación lineal, no lineal y percentiles probabilísticos. Meteorología Colombiana, 6: 121-130.

Romero, A., Ruiz de Alegría-Arzaburu, A., Rivas D., et al. 2022. Nearshore current variations during the passage of cold fronts in NW Gulf of Mexico. Continental Shelf Research, 238: 104697. doi: 10.1016/j.csr.2022.104697

Seneviratne, S.I., Zhang, X., Adnan, M., et al. 2021. Weather and climate extreme events in a changing climate. In: Masson-Delmotte, V., Zhai, P., Pirani, A., et al. (Eds.). Climate change 2012: The physical science basis. Contribution of working group I to the sixth assessment report of the intergovernmental panel on climate change. Cambridge University Press, Cambridge, pp. 1513-1766.

Torres-Pineda, C.E. & Pabón-Caicedo, J.D. 2017. Variabilidad intraestacional de la precipitación en Colombia y su relación con la oscilación de Madden-Julian. Revista de la Academia Colombiana de Ciencias Exactas y Naturales, 41: 79-93. doi: 10.18257/raccefyn.380

Van Loon, H. & Rogers, J.C. 1981. The Southern Oscillation, Part II: Associations with changes in the middle troposphere in the northern winter. Monthly Weather Review, 109: 1163-1168. doi: 10.1175/1520-0493(1981)109<1163:TSOPIA>2.0.CO;2

Zárate-Hernández, E. 2013. Climatología de masas invernales de aire frío que alcanzan Centroamérica y el Caribe y su relación con algunos índices Árticos. Tópicos Meteorológicos y Oceanográficos, 12: 35-55.

Zárate-Hernández, E. 2014. Influencia de las masas invernales de aire frío sobre el Chorro de Bajo Nivel del Caribe y sus ramas. Tópicos Meteorológicos y Oceanográficos, 13: 19-40.

Received: December 10, 2024; Accepted: April 30, 2025